Molecular mechanism of the TGF-β/Smad7 signaling pathway in ulcerative colitis

BINGQING BAI[1,2*], HUIHUI LI[2,3*], LIANG HAN[2,4], YONGYU MEI[2,5], CUI HU[1,2],
QIAO MEI[1,2], JIANMING XU[1,2] and XIAOCHANG LIU[1,2]

[1]Department of Gastroenterology; [2]The Key Laboratory of Digestive Diseases of Anhui Province,
First Affiliated Hospital of Anhui Medical University, Hefei, Anhui 230022;
[3]Department of Gastroenterology, Fuyang Cancer Hospital, Fuyang, Anhui 236010;
[4]Department of Gastroenterology, Hangzhou Ninth People's Hospital, Hangzhou, Zhejiang 311225;
[5]Department of Gastroenterology, Wuhu Second People's Hospital, Wuhu, Anhui 241000, P.R. China

Abstract. Aberrant TGF-β/Smad7 signaling has been reported to be an important mechanism underlying the pathogenesis of ulcerative colitis. Therefore, the present study aimed to investigate the effects of a number of potential anti-colitis agents on intestinal epithelial permeability and the TGF-β/Smad7 signaling pathway in an experimental model of colitis. A mouse model of colitis was first established before anti-TNF-α and 5-aminosalicylic acid (5-ASA) were administered intraperitoneally and orally, respectively. Myeloperoxidase (MPO) activity, histological index (HI) of the colon and the disease activity index (DAI) scores were then detected in each mouse. Transmission electron microscopy (TEM), immunohistochemical and functional tests, including Evans blue (EB) and FITC-dextran (FD-4) staining, were used to evaluate intestinal mucosal permeability. The expression of epithelial phenotype markers E-cadherin, occludin, zona occludens (ZO-1), TGF-β and Smad7 were measured. In addition, epithelial myosin light chain kinase (MLCK) expression and activity were measured. Anti-TNF-α and 5-ASA treatments was both found to effectively reduce the DAI score and HI, whilst decreasing colonic MPO activity, plasma levels of FD-4 and EB permeation of the intestine. Furthermore, anti-TNF-α and 5-ASA treatments decreased MLCK expression and activity, reduced

the expression of Smad7 in the small intestine epithelium, but increased the expression of TGF-β. In mice with colitis, TEM revealed partial epithelial injury in the ileum, where the number of intercellular tight junctions and the expression levels of E-cadherin, ZO-1 and occludin were decreased, all of which were alleviated by anti-TNF-α and 5-ASA treatment. In conclusion, anti-TNF-α and 5-ASA both exerted protective effects on intestinal epithelial permeability in an experimental mouse model of colitis. The underlying mechanism may be mediated at least in part by the increase in TGF-β expression and/or the reduction in Smad7 expression, which can inhibit epithelial MLCK activity and in turn reduce mucosal permeability during the pathogenesis of ulcerative colitis.

Introduction

Inflammatory bowel disease (IBD) is a chronic inflammatory disease of the gastrointestinal tract, which includes ulcerative colitis (UC) and Crohn's disease (CD). Due to the increase of prevalence of IBD and the raised mortality during the COVID-19 pandemic, IBD imposes a heavy economic and resource burden on the society (1). Therefore, it is imperative to explore the molecular mechanism of IBD and provide a new direction for its treatment. Intestinal mucosal barrier dysfunction is mainly manifested by increased intestinal mucosal permeability, which is an important pathological characteristic during the inflammatory process in IBD (2). Intestinal epithelial cells (IECs) form this barrier to which they mainly contribute two parts: Epithelial tight junction (TJ) proteins and the apical enterocyte membrane. Elevation of proinflammatory cytokine production and degradation of TJ proteins can lead to increased permeability in the intestinal mucosa during IBD (3). In addition, contraction of the intracellular actin cytoskeleton in the IECs can disrupt TJ function between cells, which opens the intercellular space to increase the permeability of the intestinal mucosa (4,5). This process also requires myosin light chain (MLC) kinase (MLCK) activity, which phosphorylates MLC (4,5). Recent studies found that promoting mucosal healing is a novel therapeutic strategy of

UC (6,7). The effects of 5-aminosalicyclic acid (5-ASA) on intestinal mucosal healing remain controversial, since there have been marked differences in outcomes among individuals (8). By contrast, salazosulfapyridine and balsalazide have been previously demonstrated to improve intestinal mucosal permeability (9). Furthermore, although anti-TNF-α therapy has been reported to confer promotional properties on mucosal healing, the specific underlying mechanism remains unclear (10).

Aberrant TGF-β/Smad7 signaling may be important for the pathogenesis of UC. In other cases, the TGF-β/Smad7 pathway has been revealed to regulate MLCK expression (11-13). However, it remains unclear if the TGF-β/Smad7 signaling pathway can regulate the expression of MLCK and intestinal mucosal permeability in the small intestine epithelium. Therefore, anti-TNF-α and 5-ASA were chosen in the present study to investigate their effects on a mouse model of dextran sulfate sodium (DSS)-induced colitis to observe their influence on intestinal permeability and the possible underlying mechanisms.

Materials and methods

Animals and reagents. A total of 32 specific pathogen-free grade C57BL/6J mice (age, 8 weeks; weight, 18-22 g; male:female, 1:1) were purchased from Shanghai SLAC Laboratory Animal Co., Ltd. They were maintained under $20\pm2°C$ temperature, 50% humidity, 12-h light/dark cycles and with tap water and a standard pellet diet. 5-ASA, anti-MLCK antibodies (cat. nos. SAB1300116-100UG and SAB1305415-40TST), FITC-dextran 4000 (FD-4; cat. no. 60842-46-8, Evans blue (EB) and DSS were purchased from Sigma-Aldrich (Merck KGaA). The Nanjing Jiancheng Biotechnology Institute supplied kits for the detection of myeloperoxidase (MPO; cat. no. A044-1-1). Anti-TNF-α (cat. no. AF-410-NA) was obtained from R&D Systems, Inc. The MLCK ELISA kit (cat. no. ELA06754) was purchased from RapidBio. Goat anti-rabbit IgG H&L (HRP; cat. no. ab205718) and primary antibodies, including anti-zona occludens (ZO-1; cat. no. ab216880), anti-E-cadherin (cat. no. ab76055), anti-occludin (cat. no. ab168986), anti-TGF-β (cat. no. ab66043) and anti-Smad7 (cat. no. ab90086) were purchased from Abcam. The RIPA buffer was obtained from Beijing Solarbio Science & Technology Co., Ltd. The SPI-PON 812 was purchased from SERVA Electrophoresis GmbH. Chloral hydrate was obtained from Shanghai Jizhi Biochemical Technology Co., Ltd. The protein concentration determination kit (BCA reagent), 10% neutral formaldehyde solution, 1% osmium acid and formamide were supplied by Beijing Solarbio Science & Technology Co., Ltd., Wuxi Zhanwang Chemical Reagent Co., Ltd., Beijing Zhongjingkeyi Technology Co., Ltd., and Shanghai Sinopharm Chemical Reagent Co., Ltd. The 25% glutaraldehyde solution (Johnson Matthey) was made into a 2.5% glutaraldehyde solution with PBS solution (pH 7.4) before use. Peroxidase blocking solution (cat. no. ZLI-9311D) and the diaminobenzidine (DAB) Color kit (cat. no. ZLI-9018) were purchased from Zsbio. Hematoxylin (cat. no. BA-4041) was supplied by Baso. TBST buffer (0.05% Tween-20; cat. no. T1085) was from Beijing Solarbio Science & Technology Co., Ltd. Analytical grade methanol,

formamide and isopropanol, NaH_2PO_4 (Mw, 119.98), NaCl (Mw, 58.44), phosphoric acid, glycerin, trichloroacetic acid, sulfosalicylic acid, isopropanol and poly-lysine slides were provided by Sinopharm Chemical Reagent Co., Ltd. Krebs solution consisted of 6.9 g NaCl, 0.35 g KCl, 0.28 g $CaCl_2$, 2.1 g $NaHCO_3$, 0.41 g $MgSO_4$ and 0.16 g KH_2PO_4. In total, 0.01 M PBS consisted of 8 g NaCl, 0.2 g KCl, 0.24 g KH_2PO_4 and 1.44 g NaH_2PO_4 dissolved in 800 ml distilled water and adjusted to pH 7.4. The following instruments were applied in the present study, including a light microscope (Olympus Corporation), Ultra-violet spectrophotometer (752N; Shanghai Precision Scientific Instruments Co., Ltd.), transmission electron microscope (TEM; Hitachi, Ltd.), microplate reader (ELx800; BioTek Instruments, Inc.) and a reverse transcription (RT)-PCR instrument (LightCycler 480; Roche Diagnostics). The Ethics Committee of Experimental Animals of Anhui Medical University (Hefei, China) approved the present study (approval no. 20150044) and experiments were conducted in accordance with laboratory animal management and use guidelines.

Induction of DSS-colitis model. A mouse colitis model was induced by 5% (w/v) DSS for 7 days of free drinking (14).

Experimental protocols. Mice were randomly classified into the normal, DSS-treated, 5-ASA-treated and anti-TNF-α-treated groups (n=8/group). Mice in the normal group did not receive DSS. The 5-ASA-treated and anti-TNF-α-treated groups were set as the treatment groups. Anti-TNF-α was administered via intraperitoneal injection at a dose of 5 mg/kg, once on day 1 and once on day 4 (15), whilst 5-ASA was administered orally at a dose of 423 mg/kg/day (16). Mice in the normal and DSS-treated groups were injected intraperitoneally with equivalent amounts of normal saline daily. All groups were treated accordingly for 7 days.

Assessment of disease activity index (DAI). In total, two observers recorded the following parameters daily: i) Body weight; ii) fecal blood; and iii) consistency. The average daily DAI score per mouse was calculated according to the standard method (14).

Assessment of inflammation. The mice were euthanized by cervical dislocation following anesthesia with 5% chloral hydrate (0.1 ml/10 g). After the use of chloral hydrate, the abdomen of the mice remained soft with no significant resistance after touch. None of the mice showed signs of peritonitis, pain or discomfort. After laparotomy, the gross mucosal morphology of mouse colon was first examined before two continuous pieces of the distal colon were collected. For histological analysis, the present study used 10% neutral buffered formalin to fix one piece of the colon at room temperature for 24 h to maintain the original morphological structure of the cell, followed by paraffin embedding for sections (thickness, 4 μm) and finally H&E staining at room temperature for 17 min. The severity of inflammation was assessed by light microscope in four aspects using the histological index (HI) (14), with a total score range of 0-14. The other piece of the colon tissue was homogenized for assessing MPO activity (17).

TEM. A 0.5-cm distal ileal segment within 1 cm of the ileocecal junction was fixed in 2.5% glutaraldehyde at 4°C for 6 h, incubated in osmic acid at 4°C for 2 h and then embedded in SPI-PON 812 for 12 h at 45°C as the specimen for TEM.

Assessment of E-cadherin, ZO-1 and occludin protein expression. Following isolation, 1 cm of the ileal tissue was fixed in 10% neutral formalin and preserved in liquid nitrogen. The expression of E-cadherin, occludin and ZO-1 in the ileal epithelial cells was detected via immunohistochemistry (IHC). Paraffin-embedded sections (4 μm) were incubated for 45 min at 60°C. Then the slices were deparaffinized in xylene, subsequently dipped in alcohol. Sections were treated with hydrogen peroxide (3%) at 37°C for 20 min, followed by incubation with goat serum (10%; cat. no. G9023; Sigma-Aldrich; Merck KGaA) at 37°C for 30 min. The primary antibodies were added 37°C for 60 min and sections were subsequently washed with PBS three times. The primary antibodies included anti-E-cadherin (1:1,000; cat. no. ab76055; Abcam), anti-zona occludens (ZO-1; 1:200; cat. no. ab216880; Abcam) and anti-occludin (1:100; cat. no. ab168986; Abcam). The slices were incubated with secondary antibodies (HRP labeled goat anti-rabbit IgG H&L; 1:5,000; cat. no. ab205718; Abcam) at 37°C for 20 min. Subsequently, the slices were exposed to diaminobenzidine for 30 sec at 37°C, counterstained with hematoxylin for 2 min at 37°C and viewed by light microscopy. JD-801 system (Jiangsu Jetta Technology Development Co., Ltd.) was used to evaluate the area and density of the staining areas, as well as the integrated optical density (IOD) values of the IHC sections. The intensity of protein staining in the image is expressed as the mean densitometry (representing relative protein expression level). Five fields were randomly selected, and the signal density of tissue area was statistically analyzed by using the blind method. To prevent false positives, negative control groups with only secondary antibodies were included. Controls with secondary antibodies were only performed while optimizing the experiments, thus these pictures are not shown in the present manuscript.

Intestinal permeability assay. According to a previously described method (18), EB and FD-4 were used to assay the intestinal permeability. A 6-cm segment of the small intestine was used as a sac by ligating both ends, before 0.2 ml 1.5% (w/v) EB dissolved in PBS was injected into the sac. The sac was then incubated in 20 ml Krebs buffer and removed after 30 min. The intestinal lumen was rinsed with physiological saline until the rinsing solution was clear and dried at 37°C for 24 h, before being weighed to obtain the dry weight of the intestinal tissue and finally incubated with formamide at 50°C for 24 h. Permeability of the intestine was assessed using EB via Ultra-violet spectrophotometer. The estimated wavelength of the dye eluting amount was 655 nm and the amount of EB was calculated according to the standard curve.

FD-4 was detected *in vivo*. The ileum of 6 cm was ligated at a distance of 2 and 8 cm from the ileocecal region after anesthesia and injected into the cavity with 0.2 ml FD-4 solution, which consisted of PBS and 25 mg/kg FD-4. The portal vein blood (100 μl) was extracted after 30 min to determine the concentration of FITC in the plasma (18).

Assessment of MLCK enzymatic activity. The intestinal mucosa homogenate was prepared at 4°C from liquid nitrogen storage after adding extract buffer. MLCK enzymatic activity in the small intestine homogenate was measured according to the protocols of the ELISA kit.

Detection of MLCK via IHC. Intestinal mucosa specimens of the ileal were collected, fixed with 10% formaldehyde overnight at room temperature and embedded in paraffin for sectioning (thickness, 4 μm). The expression of MLCK protein in the ileal epithelial cells was detected using the SP method of IHC. The experimental steps were performed according to the kit protocols. The control group was treated with PBS instead of the primary antibody. In total, three visual fields were randomly selected from each slice under the light microscope (magnification, x40) and the distribution of positive particles in the cells was observed under the light microscope (magnification, x200). To prevent false positives, negative control groups with only secondary antibodies were included. Controls with secondary antibodies were only performed while optimizing the experiments, thus these images are not included in the present manuscript.

Detection of MLCK, TGF-β and Smad7 expression via western blotting. The intestinal mucosa specimens of the ileal were cut into pieces in an ice bath and treated with the RIPA buffer to prepare the homogenate, frozen at -80°C and thawed three times to fully release the MLCK, TGF-β and Smad7. The homogenate was then centrifuged at 4°C for 15 min at 12,000 x g to extract the supernatant. Protein concentration was determined. The extract was then adjusted for protein concentration and mixed with the sample buffer for 2X protein electrophoresis and boiled for 5 min. Subsequently, the SDS-PAGE included 10% separated gel and 5% concentrated gel. Equal amounts (50 μg) of samples were loaded into each lane. After separation via SDS-PAGE, the samples were transferred onto PVDF membranes, which were then blocked and incubated with primary antibodies. After washing, the membranes were incubated with secondary antibodies before exposure after washing. BCA protein concentration determination kit was used to determine the protein concentrations. The membranes were blocked at room temperature in TBST (0.05% Tween-20) containing 5% BSA [cat. no. A600903; Sangon Biotech (Shanghai) Co., Ltd.] for 1 h and subsequently treated with primary antibodies overnight at 4°C: anti-MLCK (1:1,000; cat. no. SAB1300116 and SAB1305415; Sigma-Aldrich; Merck KGaA); anti-TGF-β (1:500; cat. no. ab66043; Abcam); anti-Smad7 (1:1,000; cat. no. ab90086-Abcam). β-actin (cat. no. 66009-1-Ig; Proteintech) was used as an endogenous control. TBST buffer was used to rinse membranes, which were treated with HRP labeled goat anti-rabbit IgG H&L (1:5,000; cat. no. ab205718; Abcam) at 37°C for 1 h. The SuperSignal® West Dura Extended Duration Substrate (cat. no. 34075; Thermo Pierce) was used to visualize the protein bands, which were detected using X-ray film (Huadong Medicine Co., Ltd.). ImageJ software version 1.8.0 (National Institutes of Health) was used to quantify the protein expression. The experiments were repeated three times.

Assessment of mRNA expression of TGF-β and Smad7. The mRNA expression levels of TGF-β and Smad7 mRNA in the IECs of the ileal were detected via RT-quantitative (q) PCR. RNA was extracted from the samples using TRIzol® (Thermo Fisher Scientific, Inc.) to establish the RT-qPCR reaction system and conditions. The samples were first mixed with TRIzol, placed in static conditions and then centrifuged at 4°C for 15 min at 12,000 x g to obtain the supernatant. The supernatant was then mixed with equal volumes of isopropanol and centrifuged at 4°C for 10 min at 12,000 x g to obtain the precipitate. These samples were washed with 75% alcohol, dried, dissolved and frozen at -80°C. The concentration, purity, quantity and quality of the RNA were all determined. cDNA samples were prepared by reverse transcription. The subsequent PCR reaction system consisted of 4 μl cDNA, 1.96 μl 10X PCR buffer, 2.4 μl MgCl$_2$ (25 mM), 1 μl upstream primer (20 pM), 1 μl downstream primer (20 pM), 0.36 μl dNTP (10 mM), 0.1 μl Taq DNA polymerase (5 IU/μl) and 10.08 μl deionized water. cDNA samples were prepared by PrimeScript™ RT Master Mix (Perfect Real Time; Takara; cat. no. RR036A) according to the manufacturer's instructions. qPCR was conducted using the TB Green Premix Ex Taq II (Tli RNaseH Plus; TAKARA; cat. no. RR820A) on a StepOnePlus Real-Time PCR System (ABI). Thermocycling conditions was as following: denaturation for 30 sec at 95°C; then 40 cycles of 5 sec at 95°C and 30 sec at 60°C. The internal references was GAPDH. The primer sequences included TGF-β, F 5'-GCG TGCTAATGGTGGAAAC-3' and R 5'-CGGTGACATCAA AAGATAACCAC-3'; Smad7, F 5'-AGAGGCTGTGTT GCTGTGAATC-3' and R 5'-GCAGAGTCGGCTAAGGTG ATG-3'; and GAPDH, F 5'-TGACTTCAACAGCGACAC CCA-3' and R 5'-CACCCTGTTGCTGTAGCCAAA-3'. All experiments were performed in triplicate. The 2$^{-\Delta\Delta Cq}$ method was used to calculate expressions of target genes (19).

Statistical analysis. Stata 16.0 software (StataCorp LP) was used to analyze ordinal variables (DAI and HI) by using the Kruskal-Wallis test followed by Dunn's post hoc test. SPSS 20.0 software (IBM Corp.) was used to analyze the other data, and one-ANOVA followed by Dunnett's post hoc test was performed to determine statistical differences between the three groups compared with the DSS group. All experiments were repeated three times. All results are presented as the mean ± standard error of the mean. P<0.05 was considered to indicate a statistically significant difference.

Results

General condition of the mice. In the DSS group, mice exhibited weight loss. At the end of the experiment, there were different degrees of blood in feces, the appearance of which was soft or thin-shaped. The DAI scores gradually increased with time (Fig. 1A). The mice in the treatment groups also showed weight loss, but the decrease was less than that of DSS group (data not shown). Meanwhile, a few mice of the treatment groups produced slightly bloody feces or positive fecal occult blood test. DAI scores of mice in the treatment groups were lower than DSS groups (P<0.05 at day 7; Fig. 1A).
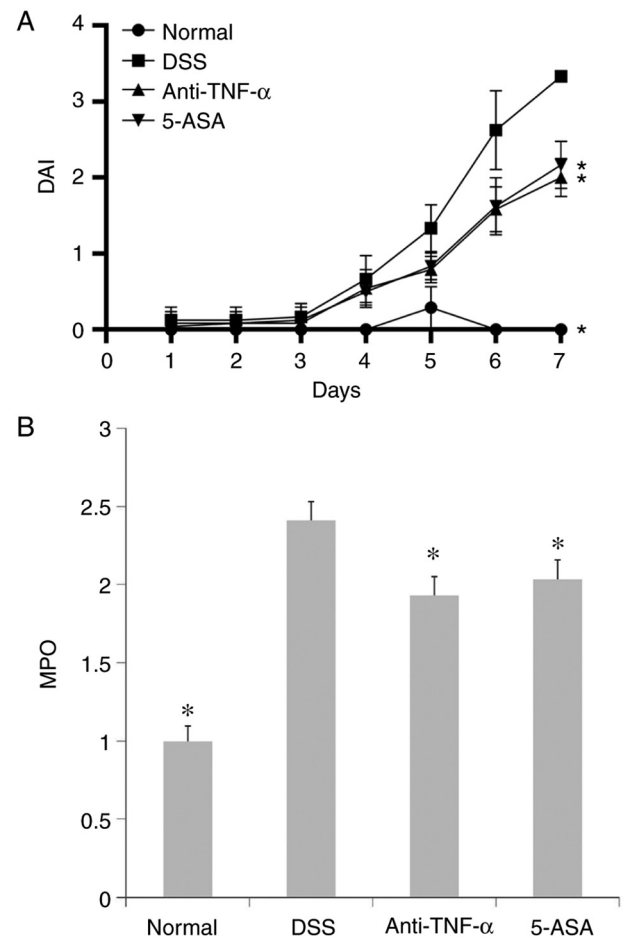

Figure 1. DAI score and MPO activity. (A) DAI score of mice in the four groups. Anti-TNF-α and 5-ASA decreased the DAI score in mice with DSS-induced colitis. (B) MPO activity in the colonic mucosa homogenates from mice in the four groups. Anti-TNF-α and 5-ASA reduced MPO activity in the colonic mucosa of mice with DSS-induced colitis. *P<0.05 vs. DSS. DAI, disease activity index; 5-ASA, 5-aminosalicylic acid; DSS, dextran sulfate sodium; MPO, myeloperoxidase.

Gross observation and pathological examination of the colonic tissue. The colon mucosa in the DSS group was characterized by extensive hyperemia and edema. In addition, multiple erosion, bleeding spots and superficial ulcers were observed (data not shown). However, no obvious abnormalities could be found in tissues from mice in the normal group. By contrast, only scattered hyperemia and erosion were observed without obvious bleeding or ulcers in treatment groups.

H&E pathological examination revealed that in the DSS group, the colonic mucosa had multiple superficial ulcers, where a large number of the crypt glands were destroyed with extensive inflammatory cell infiltration (Fig. 2A). By contrast, in the normal group the colonic IECs remained intact such that the crypt glands were neatly arranged with no inflammatory cell infiltration (Fig. 2B). In the two treatment groups, colon mucosal tissues from only a few mice exhibited superficial ulcers, where there were also signs of crypt gland destruction compared with that of the normal group. However, the extent of ulceration and crypt destruction was markedly lower compared with that in the DSS group. Additionally, the degree of infiltration by inflammatory cells in the mucosa and submucosa was mild in treatment groups (Fig. 2C and D). Compared
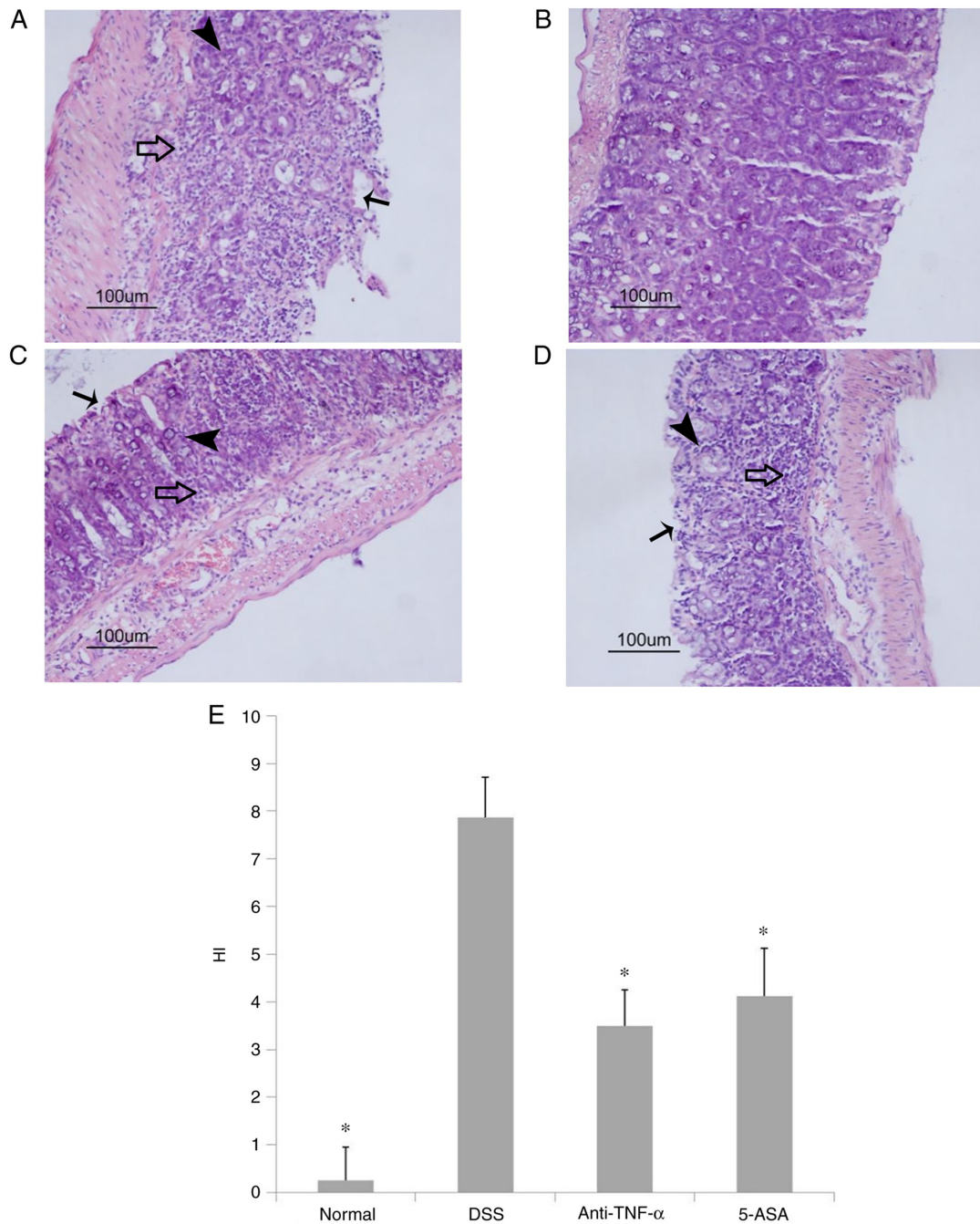
Figure 2. Histology and HI score of the colon. Histology of the mice colon in the (A) DSS, (B) normal, (C) anti-TNF-α and (D) 5-ASA groups as assessed by H&E staining. Magnification, x200. Arrows indicate crypts, long-tailed arrows indicate erosion or ulcerated intestinal mucosa, and hollow arrows indicate inflammatory cell infiltration. (E) HI score of the mouse colonic mucosa in the four groups. Anti-TNF-α and 5-ASA decreased the HI score of the colonic mucosa in mice with DSS-induced colitis. *P<0.05 vs. DSS. DSS, dextran sulfate sodium; HI, histological index; 5-ASA, 5-aminosalicyclic acid.

with those in the DSS group, the HI scores in the treated groups were significantly lower (P<0.05; Fig. 2E).

MPO activity in the colon. The activity of MPO in the colonic homogenates from the DSS group was higher compared with that in the normal group, whilst the MPO activity in the treatment groups was decreased compared with that in the DSS group. This suggested that the degree of colon inflammation in the DSS group was significant (P<0.05; Fig. 1B), which could be alleviated by anti-TNF-α and 5-ASA treatment (P<0.05; Fig. 1B).

Ultrastructure of the intestinal mucosal barrier. TEM was used to observe the ultrastructure of the IECs in the ileum of mice. It was observed that in the normal group, the IECs within the tissue were intact, where the surface microvilli were long and dense and the arrangement was regular. The cells were also closely connected. However, in the DSS group, edema or even shedding of IECs could be observed, which was accompanied by atrophy and sparseness of the surface microvilli, enlargement of the intercellular space and the opening of a number of TJs. In the treatment groups, although edema of some IECs, reduction of the number of microvilli and the
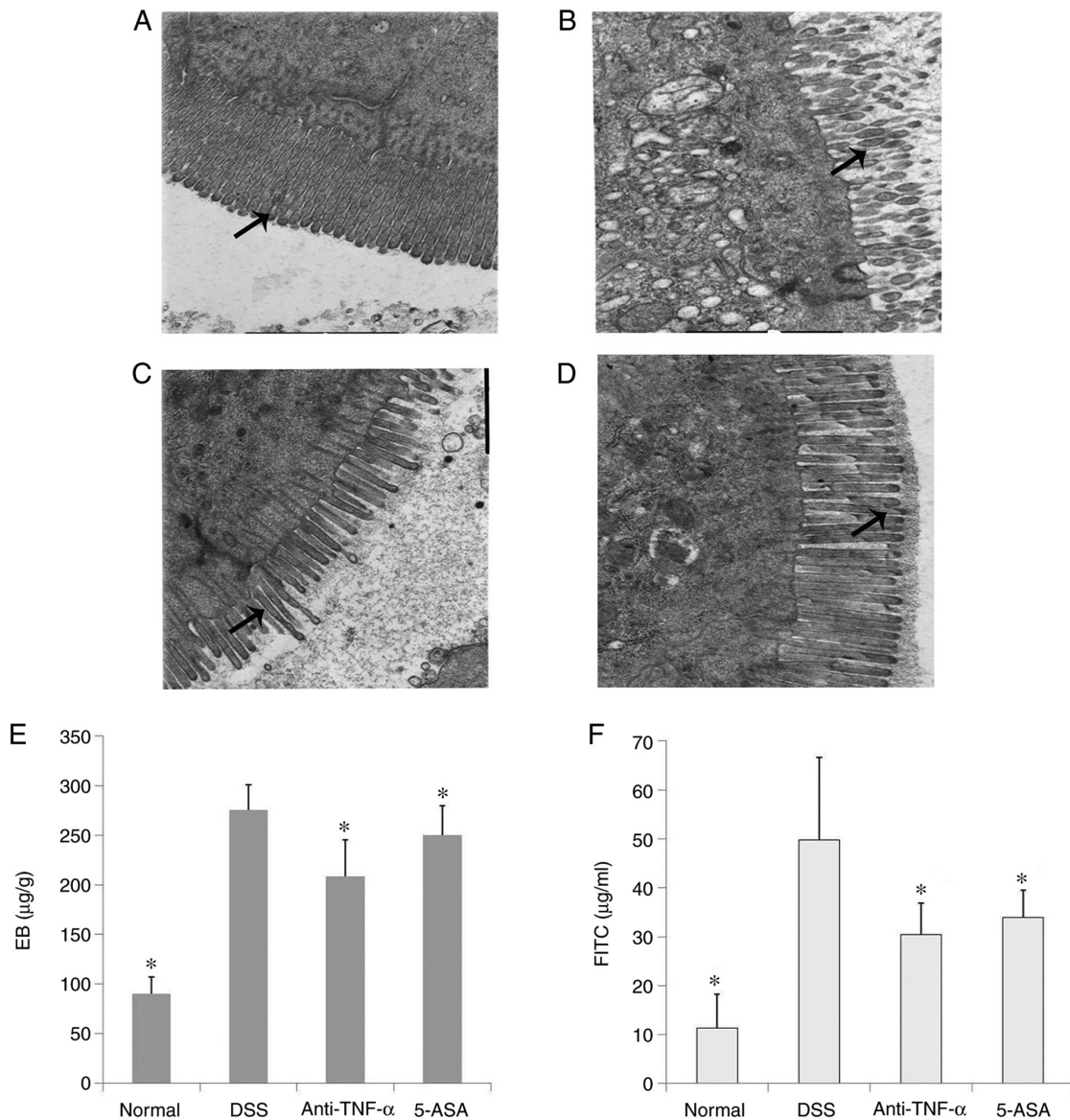
Figure 3. Ultrastructure and function detection of the intestine. Ultrastructure of the intestinal mucosal barrier as observed by transmission electron micros-copy in the (A) normal, (B) DSS, (C) anti-TNF-α and (D) 5-ASA groups. Magnification, x20,000. Long-tailed arrows indicate surface microvilli. (E) The amount of EB permeating into the intestine isolated from mice in each of the four groups. Anti-TNF-α and 5-ASA decreased the level of intestinal EB staining in mice with DSS-induced colitis. (F) Plasma FITC-dextran 4000 level of the four groups. Anti-TNF-α and 5-ASA decreased the level of blood FITC in mice with DSS-induced colitis *$P<0.05$ vs. DSS. DSS, dextran sulfate sodium; EB, Evans blue; 5-ASA, 5-aminosalicyclic acid.

opening of TJs could also be observed, the severity was lower compared with that in the DSS group (Fig. 3A-D).

Intestinal mucosal barrier function. Compared with those in the normal group, the intestinal EB content and plasma FITC levels in the DSS group were significantly increased ($P<0.05$; Fig. 3E and F). This suggested that the intestinal mucosal barrier in DSS group was damaged, which allowed the high molecular weight EB to enter the intestinal mucosa through the expanded TJs, which could also have resulted in the absorption of FITC into the portal vein system. Anti-TNF-α and 5-ASA treatment could significantly decrease the level of intestinal EB and plasma FITC by varying degrees ($P<0.05$; Fig. 3E and F).

Protein expression of TJs and adhesion junctions (AJs). According to the results of IHC, it was found that the expression of occludin, ZO-1 and E-cadherin in the small intestinal mucosal epithelial cells of mice in the treated groups were lower compared with those in the control group, but were higher compared with those in the DSS group (Figs. 4-6 and Table I).

Expression, distribution and activity of the MLCK protein. The expression and activity of the MLCK protein in small intestinal mucosal epithelial cells were higher in the DSS group compared with those in the normal group, but were lower in the treated group compared with those in the DSS group ($P<0.05$; Fig. 7). The results of IHC (Fig. 7A and Table I) were consistent with those observed following western blot-ting (Fig. 7B). Although there were significant differences in MLCK expression and activity between the treatment and DSS groups ($P<0.05$; Fig. 7C).

Table I. Mean density of occludin, ZO-1, E-cadherin and MLCK in different groups according to the results of immunohistochemistry.

Groups	Occludin	ZO-1	E-cadherin	MLCK
Normal	0.331	0.429	0.321	0.333
DSS	0.295	0.300	0.192	0.370
Anti-TNF-α	0.316	0.336	0.283	0.348
5-ASA	0.308	0.309	0.248	0.353

5-ASA, 5-aminosalicyclic acid; DSS, dextran sulfate sodium; ZO-1, zona occludens-1; MLCK, myosin light chain kinase.
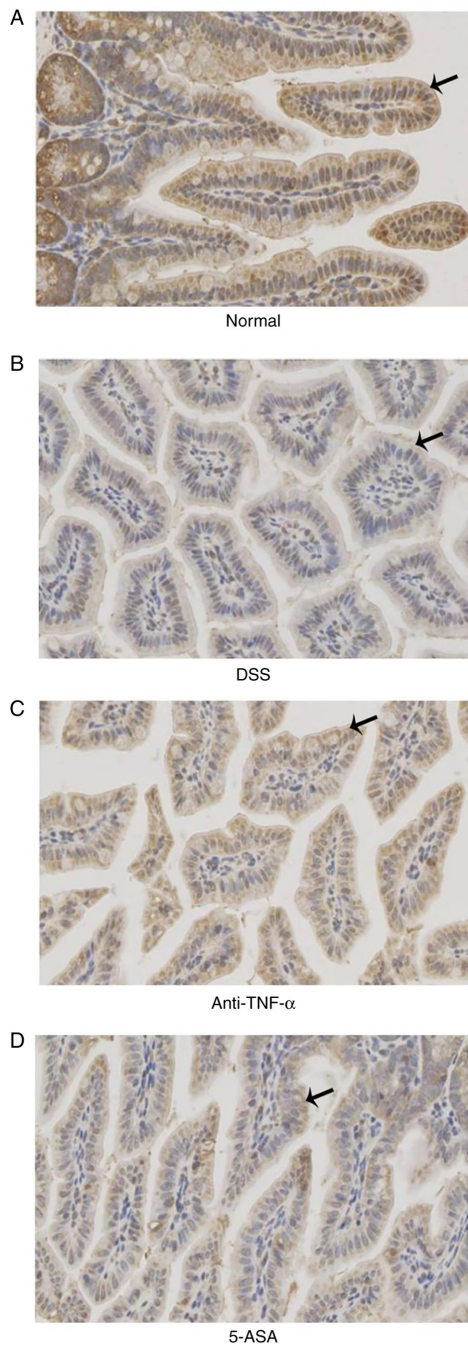

Figure 4. Expression of occludin in the intestinal epithelium as observed via immunohistochemistry. Occludin expression in the (A) normal, (B) DSS, (C) anti-TNF-α and (D) 5-ASA groups. Anti-TNF-α and 5-ASA increased the expression of occludin in the intestinal epithelium of mice with DSS-induced colitis. Long-tailed arrows indicate Occludin expression. DSS, dextran sulfate sodium; 5-ASA, 5-aminosalicyclic acid.
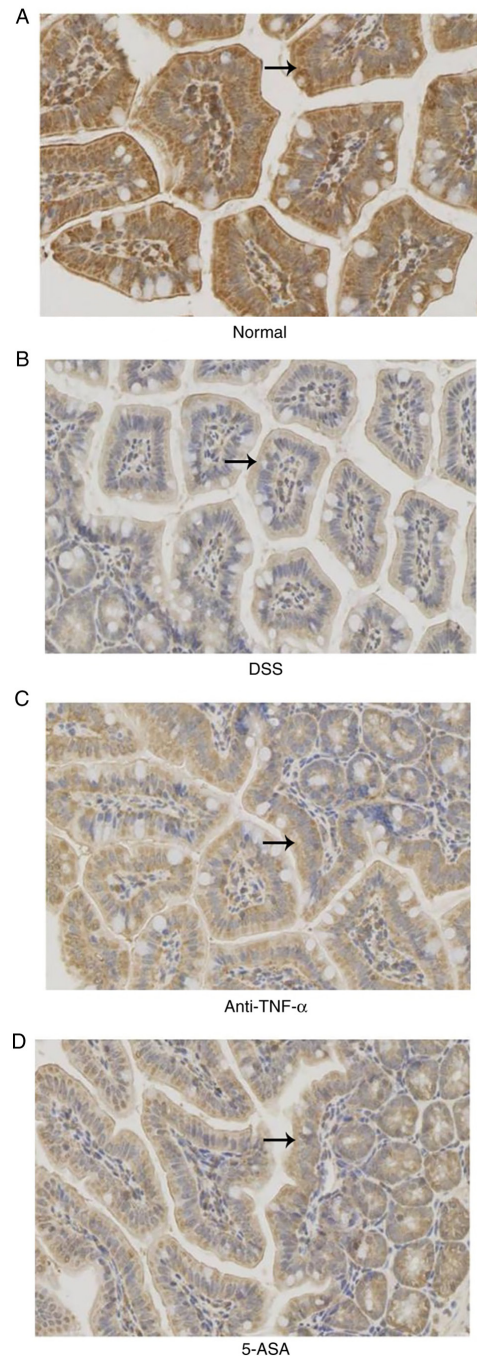

Figure 5. Expression of ZO-1 in the intestinal epithelium as observed via immunohistochemistry. ZO-1 expression in the (A) normal, (B) DSS, (C) anti-TNF-α and (D) 5-ASA groups. Anti-TNF-α and 5-ASA increased the expression of ZO-1 in the intestinal epithelium of mice with DSS-induced colitis. Long-tailed arrows indicate ZO-1 expression. DSS, dextran sulfate sodium; 5-ASA, 5-aminosalicyclic acid; ZO-1, zona occludens-1.
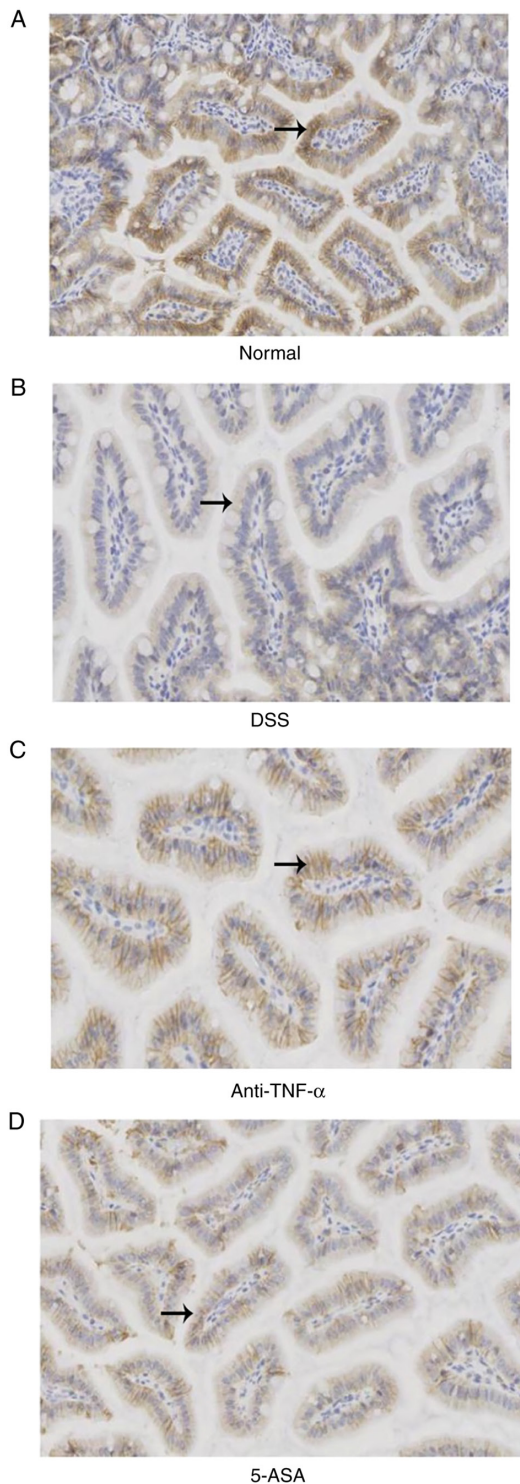
Figure 6. Expression of E-cadherin in the intestinal epithelium was observed via immunohistochemistry. E-cadherin expression in the (A) normal, (B) DSS, (C) anti-TNF-α and (D) 5-ASA groups. Anti-TNF-α and 5-ASA improved the expression of E-cadherin in the intestinal epithelium of mice with DSS-induced colitis. Long-tailed arrows indicate E-cadherin expression. DSS, dextran sulfate sodium; 5-ASA, 5-aminosalicylic acid.

mRNA and protein expression of TGF-β and Smad7. Compared with those in the normal group, the mRNA and protein expression levels of TGF-β and Smad7 were decreased and increased in the DSS group, respectively. Intervention with anti-TNF-α and 5-ASA reversed the aforementioned effects mediated by DSS (P<0.05, Fig. 8A and B). The purity
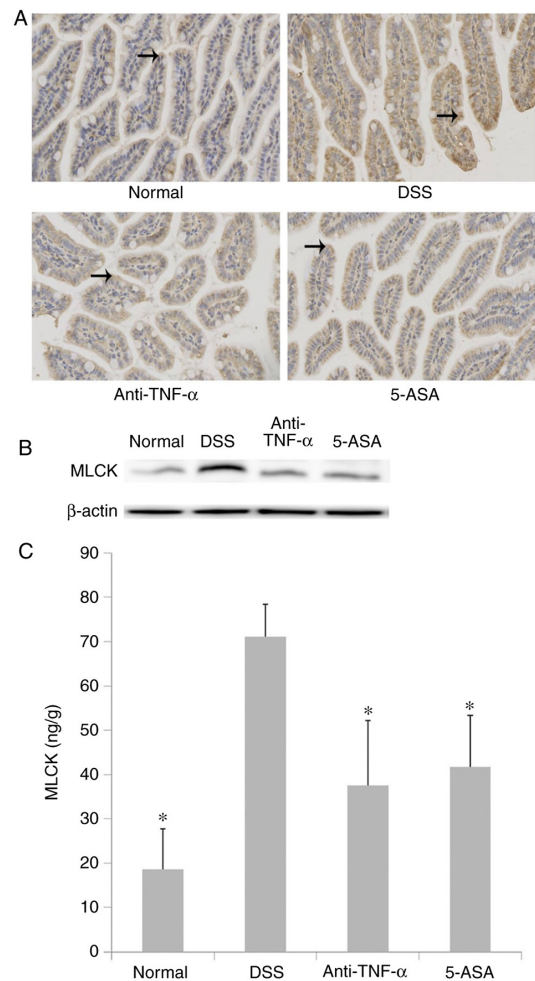

Figure 7. Expression, distribution and activity of MLCK. (A) Expression and distribution of MLCK protein expression in the intestinal epithelium as observed via IHC. Anti-TNF-α and 5-ASA decreased the expression of MLCK protein in the intestinal epithelium of mice with DSS-induced colitis. Long-tailed arrows indicate MLCK expression. (B) The expression of MLCK in the intestinal epithelium as detected via western blotting. The results of western blotting were consistent with those in IHC. (C) MLCK enzymatic activity in the intestinal epithelium as detected by using ELISA. Anti-TNF-α and 5-ASA decreased MLCK enzymatic activity in the intestinal epithelium of mice with DSS-induced colitis. However, no significant difference was detected between anti-TNF-α and 5-ASA. *P<0.05 vs. DSS. MLCK, myosin light chain kinase; IHC, immunohistochemistry; DSS, dextran sulfate sodium; 5-ASA, 5-aminosalicyclic acid.

of TGF-β1 RNA was between 1.86-1.98, whereas the concentration was 843.6-1421.6 µg/µl (data not shown). The purity of Smad7 RNA was between 1.86-1.97, whilst the concentration was 821.3-1895.8 µg/µl.

Discussion

UC is a recurrent, non-specific inflammatory disease. Intestinal mucosal barrier damage may be an important cause for the onset and recurrence of UC (2). Previous studies on human samples and animal models found that intestinal mucosal permeability increased significantly before the manifestation of intestinal inflammation (20,21).

In the present study, anti-TNF-α and 5-ASA were found to improve the clinical symptoms of UC, reduce the DAI and colonic mucosal HI scores and decrease MPO activity
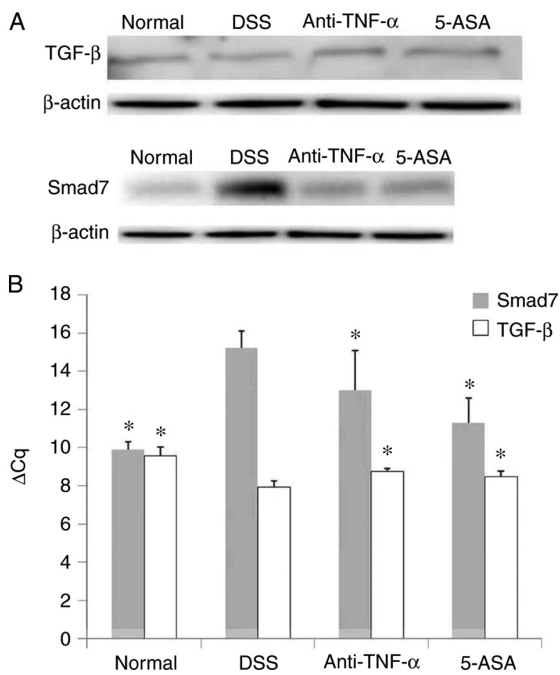
Figure 8. Protein and mRNA expression of both TGF-β and Smad7. (A) Protein expression of TGF-β and Smad7 in the intestinal epithelium was detected by western blotting. In mice with DSS-induced colitis treated with anti-TNF-α and 5-ASA, TGF-β and Smad7 expression were increased and decreased, respectively. (B) TGF-β and Smad7 mRNA expression in the intestinal epithelium were detected by reverse transcription-quantitative PCR. In mice with DSS-induced colitis treated with anti-TNF-α and 5-ASA, TGF-β and Smad7 mRNA expression were increased and decreased, respectively. *$P<0.05$ vs. DSS. DSS, dextran sulfate sodium; 5-ASA, 5-aminosalicylic acid.

in mice with DSS-induced UC, suggesting that anti-TNF-α and 5-ASA could alleviate inflammatory injury in the colon. Subsequently, TEM was used to observe the ultrastructure in the small intestine, and EB and FITC were used to detect the permeability of the small intestinal mucosa. Although TEM results suggested that anti-TNF-α and 5-ASA could improve the structure and function of the small intestinal mucosa, their specific mechanism remains unclear.

TJs are expressed at the top of the IECs, the components of which include occludin, claudin, ZO and junction adhesion molecule (JAM)-1 (22). The AJ is a structure that lies adjacent to TJs, which includes E-cadherin and β-catenin. In transgenic animal models, absence of E-cadherin expression can result in the dysfunction of AJs during the pathophysiological process of IBD (21). By blocking the adjacent intercellular spaces within the intestinal epithelium, TJs can prevent bacteria, antigens and other harmful substances from entering the intestinal mucosal lamina propria to activate immune cells (23). TJ assembly is largely dependent on AJ formation (9,24). Previously, it was found that a number of IBD-associated loci could regulate the expression of E-cadherin and stability of AJs (25,26), where it was subsequently confirmed genetically that TJs and AJs both serve a role in intestinal barrier function (25,26). In the present study, the expression of occludin, ZO-1 and E-cadherin in the mucosal epithelium of the small intestine of mice with DSS was decreased. Consistent with these results from the present study, Clayburgh et al (5) found that in patients with IBD, TJs were significantly damaged, which increased the permeability of the intestinal mucosa.

TNF-α treatment has been reported to lead to the internalization and disruption of junctional proteins, such as occludin and E-cadherin. Following 5-ASA pretreatment, membranous localization of proteins of TJs and AJs was maintained (9). In addition, 5-ASA could increase intercellular adhesion through the restoration of AJ proteins onto the cell membrane, such as β-catenin and E-cadherin, in turn promoting mucosal healing. 5-ASA can also alter the transcriptional regulation of proteins, including JAMs, claudins and epithelial cytoskeletal proteins (9). The present study also found that 5-ASA increased the expression of occludin, ZO-1 and E-cadherin in the intestinal mucosal epithelium of DSS mice.

Anti-TNF-α has been documented to decrease neutrophil infiltration in inflammatory mucosa of patients with IBD and reduce the activity of T cells and inflammatory mediators (27,28). In addition, anti-TNF-α can inhibit neutrophils from producing proinflammatory mediators, including reactive oxygen species, TNF-α and IL-8 (27,28). In particular, by binding to the antibody, TNF-α receptor activation is blocked, leading to the reduction of intestinal permeability due to the decrease in paracellular permeability across the TJs and decreased apoptosis of IECs (28). The present study showed that anti-TNF-α increased the expression of occludin, ZO-1 and E-cadherin in the epithelium of small intestinal mucosa from mice with DSS.

The degree of MLC phosphorylation depends on the activity of MLCK (4). TNF-α has been previously found to upregulate the distribution and expression of NF-κB p65 (29-31). NF-κB can bind to the promoter region of the MLCK gene to increase its transcription (31). By contrast, 5-ASA has been reported to regulate intestinal epithelial homeostasis by inhibiting the ERK1/2, Wnt/β-catenin and NF-κB signaling pathways, whilst inducing cell cycle arrest (31). In addition, 5-ASA pretreatment was revealed to alleviate the increase in NF-κB p65 mediated by TNF-α (9). Blair et al (32) previously documented that the expression of MLCK in IECs of 26 patients with IBD was increased according to the results of an immunofluorescence assay. However, since intestinal mucosal permeability was not simultaneously measured, the potential association between MLCK and intestinal mucosal barrier function could not be proven. In the present study, the expression, distribution and activity of the MLCK protein in IECs were also measured. Compared with that in the normal group, the expression of MLCK in the DSS group was increased and the activity was enhanced. Intervention with anti-TNF-α and 5-ASA could decrease the expression and activity of MLCK, which could reduce the permeability of the intestinal mucosa in mice with UC. However, no significant difference between anti-TNF-α and 5-ASA could be observed.

Aberrant TGF-β/Smad7 signaling may be an important mechanism of IBD. In particular, increased expression of Smad7 and the imbalance in the homeostasis between Smad7, Smad2 and Smad3 can lead to the loss of the anti-inflammatory effects of TGF-β, resulting in chronic inflammation in the intestinal tract during UC (33). Abnormalities in TGF-β and TGF-β receptor 2 are key to the pathogenesis of IBD. TGF-β can maintain the integrity of the tissue structure by regulating the proliferation and differentiation of T lymphocytes (33).

There is evidence that during the active stage of IBD, the number of regulatory T (Treg) cells, which regulate lymphocyte activity by secreting anti-inflammatory cytokines, such as IL-10 and TGF-β, is lower compared with that in healthy individuals (34). Treg cell disorders, which are of importance to the development of various diseases, can maintain the vicious cycle of inflammation and disease aggravation, resulting in impaired barrier function (35). Anti-TNF-α has been shown to upregulate the number of Treg cells (28). In addition, Smad7 induced by TGF-β is considered to be one of the key negative regulatory factors in the TGF-β/Smad signal transduction pathway. Activated Smad7 can inhibit the phosphorylation and activation of Smad2/3 by binding to TGF-β receptor 1, in addition to accelerating its inactivation by activating protein phosphatase PP1 and degradation by the ubiquitin ligase SMAD-specific E3 ubiquitin protein ligase 2 (36). Furthermore, Smad7 can enter the nucleus and block Smad2-3/Smad4 complex binding to target genes (37). The level of Smad7 expression is the main regulatory factor for determining TGF-β transcription (36). Knockdown of Smad7 expression was found to enhance endogenous TGF-β signaling (38). Increased expression of TGF-β in the colon was previously shown in various murine colitis models and patients with UC (39). Sedda et al (40) revealed that, although the production of TGF-β1 is increased, deficiency in the TGF-β1/Smad signaling pathway sustains the chronic inflammation of IBD. However, in the present study, TGF-β was mainly studied in the small intestine, which showed that TGF-β mRNA and protein expression in the DSS group was reduced. Consistent with these results, Vieira et al (41) also found a reduction in TGF-β expression in the duodenum of mice with DSS.

A previous study reported that Smad7 inhibition in patients with CD conferred endoscopic and clinical improvements during phase 1 and 2 clinical trials (42). However, the corresponding phase 3 trial was suspended due to the lack of efficacy (43). A recent study has indicated that rigorous experimental design assist in furthering the understanding in the significance of Smad7 as a therapeutic target for IBD (36). In addition, Wu-Mei-Wan is a classic Chinese medicine for treating digestive diseases and pervious study has shown that the antifibrotic effects of it may result from the inhibition of the TGF-β/Smad pathway (44), whilst knocking down Smad7 expression was found to be beneficial in preventing the post-operative recurrence of CD (45). Therefore, understanding the molecular characteristics of IBD will assist in the identification of novel candidates for the inhibition of Smad7. Nevertheless, the mechanism of Smad7 in IBD remains to be fully elucidated (43,46).

In the present study, compared with that in the normal group, Smad7 protein and mRNA expression was increased in the IECs of mice with DSS. This was consistent with findings from previous studies. Monteleone et al (47) showed that the levels of phosphorylated Smad3 in lamina propria mononuclear cells in the intestinal mucosa were significantly decreased, whereas Smad7 expression was markedly increased in patients with CD and UC compared with those in the normal group. It has been suggested that the overexpression of Smad7 can inhibit the TGF-β signaling pathway, where inflammatory cytokines in the intestinal mucosa, such as TNF-α and IFN-γ, can be continuously increased during IBD (48). In addition, IFN-γ can inhibit the TGF-β/Smad signaling pathway by upregulating the expression of Smad7, whilst TNF-α can directly interfere with the formation of the Smad2/3-Smad4 complex with DNA through the inducible protein activator (49,50). However, Monteleone et al (51) analyzed the expression of Smad7 in the mucosal samples from patients with IBD and found that Smad7 expression was increased at the protein levels, but not the mRNA levels, suggesting the post-transcriptional regulation of Smad7. The mucous membrane specimens of patients with UC in this previous study were mainly taken from the colon, whilst the present study was performed on the small intestine. Intervention with anti-TNF-α and 5-ASA was demonstrated to increase the expression of TGF-β whilst weakening Smad7, suggesting that both may regulate MLCK activity through the TGF-β/Smad7 signaling pathway. This in turn can alter the expression levels of TJ and AJ proteins in IECs before finally regulating intestinal permeability.

To conclude, the present study evaluated the effects of anti-TNF-α and 5-ASA on the TGF-β/Smad7 signaling pathway in a mouse experimental model of colitis. Similar studies were performed in the colon (40,52-57), peripheral blood (58) or in chronic pathologies (53,56), whereas the present experiment studied the small intestine and acute response to injury. It was found that anti-TNF-α and 5-ASA both improved the permeability of the intestinal epithelium on this model of UC. The mechanism was partly due to the increase in TGF-β expression or the decrease in Smad7 expression, which may inhibit epithelial MLCK expression and activity, leading to the reduction of intestinal mucosal permeability in UC. The present study may provide novel evidence for the treatment of IBD by either upregulating TGF-β expression or downregulating Smad7 expression.

Availability of data and materials

The datasets used and/or analyzed during the current study are available from the corresponding author on reasonable request.

Authors' contributions

BB designed and performed the experiments and data interpretation. HL performed experiments and data analysis. BB and HL wrote and revised the manuscript. LH, YM and CH assisted in the completion of animal experiments and some molecular biology experiments. QM and XL designed and guided all experiments. JX assisted in guiding experimental design and data analysis. BB, HL and XL confirm the authenticity of all the raw data. All authors have read and approved the final manuscript.

Ethics approval and consent to participate

The Ethics Committee of Experimental Animals of Anhui Medical University (Hefei, China) approved the present study (approval no. 20150044) and experiments were conducted in accordance with laboratory animal management and use guidelines.

Patient consent for publication

Not applicable.

Competing interests

The authors declare that they have no competing interests.

References

1. Kaplan GG and Windsor JW: The four epidemiological stages in the global evolution of inflammatory bowel disease. Nat Rev Gastroenterol Hepatol 18: 56-66, 2021.
2. Ramos GP and Papadakis KA: Mechanisms of disease: Inflammatory bowel diseases. Mayo Clin Proc 94: 155-165, 2019.
3. Vergnolle N: Protease inhibition as new therapeutic strategy for GI diseases. Gut 65: 1215-1224, 2016.
4. Huang S, Fu Y, Xu B, Liu C, Wang Q, Luo S, Nong F, Wang X, Huang S, Chen J, et al: Wogonoside alleviates colitis by improving intestinal epithelial barrier function via the MLCK/pMLC2 pathway. Phytomedicine 68: 153179, 2020.
5. Clayburgh DR, Shen L and Turner JR: A porous defense: The leaky epithelial barrier in intestinal disease. Lab Invest 84: 282-291, 2004.
6. Li K, Marano C, Zhang H, Yang F, Sandborn WJ, Sands BE, Feagan BG, Rubin DT, Peyrin-Biroulet L, Friedman JR and De Hertogh G: Relationship between combined histologic and endoscopic endpoints and efficacy of ustekinumab treatment in patients with ulcerative colitis. Gastroenterology 159: 2052-2064, 2020.
7. Ungaro R, Colombel JF, Lissoos T and Peyrin-Biroulet L: A treat-to-target update in ulcerative colitis: A systematic review. Am J Gastroenterol 114: 874-883, 2019.
8. Rubin DT, Ananthakrishnan AN, Siegel CA, Sauer BG and Long MD: ACG clinical guideline: Ulcerative colitis in adults. Am J Gastroenterol 114: 384-413, 2019.
9. Khare V, Krnjic A, Frick A, Gmainer C, Asboth M, Jimenez K, Lang M, Baumgartner M, Evstatiev R and Gasche C: Mesalamine and azathioprine modulate junctional complexes and restore epithelial barrier function in intestinal inflammation. Sci Rep 9: 2842, 2019.
10. Scarallo L, Bolasco G, Barp J, Bianconi M, di Paola M, Di Toma M, Naldini S, Paci M, Renzo S, Labriola F, et al: Anti-tumor necrosis factor-alpha withdrawal in children with inflammatory bowel disease in endoscopic and histologic remission. Inflamm Bowel Dis: Apr 9, 2021 (Epub ahead of print).
11. Yang H, Zhang L, Weakley SM, Lin PH, Yao Q and Chen C: Transforming growth factor-beta increases the expression of vascular smooth muscle cell markers in human multi-lineage progenitor cells. Med Sci Monit 17: BR55-BR61, 2011.
12. Zhu B, Zhai J, Zhu H and Kyprianou N: Prohibitin regulates TGF-beta induced apoptosis as a downstream effector of Smad-dependent and -independent signaling. Prostate 70: 17-26, 2010.
13. Sinpitaksakul SN, Pimkhaokham A, Sanchavanakit N and Pavasant P: TGF-beta1 induced MMP-9 expression in HNSCC cell lines via Smad/MLCK pathway. Biochem Biophys Res Commun 371: 713-718, 2008.
14. Kihara N, de la Fuente SG, Fujino K, Takahashi T, Pappas TN and Mantyh CR: Vanilloid receptor-1 containing primary sensory neurones mediate dextran sulphate sodium induced colitis in rats. Gut 52: 713-719, 2003.
15. Scheinin T, Butler DM, Salway F, Scallon B and Feldmann M: Validation of the interleukin-10 knockout mouse model of colitis: Antitumour necrosis factor-antibodies suppress the progression of colitis. Clin Exp Immunol 133: 38-43, 2003.
16. Liu XC, Mei Q, Xu JM and Hu J: Balsalazine decreases intestinal mucosal permeability of dextran sulfate sodium-induced colitis in mice. Acta Pharmacol Sin 30: 987-993, 2009.
17. Kannengiesser K, Maaser C, Heidemann J, Luegering A, Ross M, Brzoska T, Bohm M, Luger TA, Domschke W and Kucharzik T: Melanocortin-derived tripeptide KPV has anti-inflammatory potential in murine models of inflammatory bowel disease. Inflamm Bowel Dis 14: 324-331, 2008.
18. Liu X, Xu J, Mei Q, Han L and Huang J: Myosin light chain kinase inhibitor inhibits dextran sulfate sodium-induced colitis in mice. Dig Dis Sci 58: 107-114, 2013.
19. Livak KJ and Schmittgen TD: Analysis of relative gene expression data using real-time quantitative PCR and the 2(-Delta Delta C(T)) method. Methods 25: 402-408, 2001.
20. Arrieta MC, Madsen K, Doyle J and Meddings J: Reducing small intestinal permeability attenuates colitis in the IL10 gene-deficient mouse. Gut 58: 41-48, 2009.
21. Martini E, Krug SM, Siegmund B, Neurath MF and Becker C: Mend your fences: The epithelial barrier and its relationship with mucosal immunity in inflammatory bowel disease. Cell Mol Gastroenterol Hepatol 4: 33-46, 2017.
22. Buckley A and Turner JR: Cell biology of tight junction barrier regulation and mucosal disease. Cold Spring Harb Perspect Biol 10: a029314, 2018.
23. Otani T and Furuse M: Tight junction structure and function revisited: (Trends in cell biology 30, 805-817, 2020). Trends Cell Biol 30: 1014, 2020.
24. Rajasekaran AK, Hojo M, Huima T and Rodriguez-Boulan E: Catenins and zonula occludens-1 form a complex during early stages in the assembly of tight junctions. J Cell Biol 132: 451-463, 1996.
25. Mohanan V, Nakata T, Desch AN, Lévesque C, Boroughs A, Guzman G, Cao Z, Creasey E, Yao J, Boucher G, et al: C1orf106 is a colitis risk gene that regulates stability of epithelial adherens junctions. Science 359: 1161-1166, 2018.
26. UK IBD Genetics Consortium; Barrett JC, Lee JC, Lees CW, Prescott NJ, Anderson CA, Phillips A, Wesley E, Parnell K, Zhang H, et al: Genome-wide association study of ulcerative colitis identifies three new susceptibility loci, including the HNF4A region. Nat Genet 41: 1330-1334, 2009.
27. Zhang C, Shu W, Zhou G, Lin J, Chu F, Wu H and Liu Z: Anti-TNF-α therapy suppresses proinflammatory activities of mucosal neutrophils in inflammatory bowel disease. Mediators Inflamm 2018: 3021863, 2018.
28. Olesen CM, Coskun M, Peyrin-Biroulet L and Nielsen OH: Mechanisms behind efficacy of tumor necrosis factor inhibitors in inflammatory bowel diseases. Pharmacol Ther 159: 110-119, 2016.
29. Al-Sadi R, Guo S, Ye D, Rawat M and Ma TY: TNF-α modulation of intestinal tight junction permeability is mediated by NIK/IKK-α axis activation of the canonical NF-κB pathway. Am J Pathol 186: 1151-1165, 2016.
30. Chen S, Zhu J, Chen G, Zuo S, Zhang J, Chen Z, Wang X, Li J, Liu Y and Wang P: 1,25-Dihydroxyvitamin D3 preserves intestinal epithelial barrier function from TNF-α induced injury via suppression of NF-kB p65 mediated MLCK-P-MLC signaling pathway. Biochem Biophys Res Commun 460: 873-878, 2015.
31. Ye D and Ma TY: Cellular and molecular mechanisms that mediate basal and tumour necrosis factor-alpha-induced regulation of myosin light chain kinase gene activity. J Cell Mol Med 12: 1331-1346, 2008.
32. Blair SA, Kane SV, Clayburgh DR and Turner JR: Epithelial myosin light chain kinase expression and activity are upregulated in inflammatory bowel disease. Lab Invest 86: 191-201, 2006.
33. Stolfi C, Troncone E, Marafini I and Monteleone G: Role of TGF-beta and Smad7 in gut inflammation, fibrosis and cancer. Biomolecules 11: 17, 2020.
34. Maul J, Loddenkemper C, Mundt P, Berg E, Giese T, Stallmach A, Zeitz M and Duchmann R: Peripheral and intestinal regulatory CD4+ CD25(high) T cells in inflammatory bowel disease. Gastroenterology 128: 1868-1878, 2005.
35. Fan L, Qi Y, Qu S, Chen X, Li A, Hendi M, Xu C, Wang L, Hou T, Si J and Chen S: B. adolescentis ameliorates chronic colitis by regulating Treg/Th2 response and gut microbiota remodeling. Gut Microbes 13: 1-17, 2021.
36. de Ceuninck van Capelle C, Spit M and Ten Dijke P: Current perspectives on inhibitory SMAD7 in health and disease. Crit Rev Biochem Mol Biol 55: 691-715, 2020.
37. Zhang S, Fei T, Zhang L, Zhang R, Chen F, Ning Y, Han Y, Feng XH, Meng A and Chen YG: Smad7 antagonizes transforming growth factor beta signaling in the nucleus by interfering with functional Smad-DNA complex formation. Mol Cell Biol 27: 4488-4499, 2007.

38. Fantini MC, Rizzo A, Fina D, Caruso R, Sarra M, Stolfi C, Becker C, Macdonald TT, Pallone F, Neurath MF and Monteleone G: Smad7 controls resistance of colitogenic T cells to regulatory T cell-mediated suppression. Gastroenterology 136: 1308-1316, e1-e3, 2009.

39. Olsen T, Rismo R, Cui G, Goll R, Christiansen I and Florholmen J: TH1 and TH17 interactions in untreated inflamed mucosa of inflammatory bowel disease, and their potential to mediate the inflammation. Cytokine 56: 633-640, 2011.

40. Sedda S, Marafini I, Dinallo V, Di Fusco D and Monteleone G: The TGF-β/Smad system in IBD pathogenesis. Inflamm Bowel Dis 21: 2921-2925, 2015.

41. Vieira EL, Leonel AJ, Sad AP, Beltrão NR, Costa TF, Ferreira TM, Gomes-Santos AC, Faria AM, Peluzio MC, Cara DC and Alvarez-Leite JI: Oral administration of sodium butyrate attenuates inflammation and mucosal lesion in experimental acute ulcerative colitis. J Nutr Biochem 23: 430-436, 2012.

42. Ardizzone S, Bevivino G and Monteleone G: Mongersen, an oral Smad7 antisense oligonucleotide, in patients with active Crohn's disease. Therap Adv Gastroenterol 9: 527-532, 2016.

43. Feagan BG, Sands BE, Rossiter G, Li X, Usiskin K, Zhan X and Colombel JF: Effects of mongersen (GED-0301) on endoscopic and clinical outcomes in patients with active Crohn's disease. Gastroenterology 154: 61-64.e6, 2018.

44. Wu F, Shao Q, Hu M, Zhao Y, Dong R, Fang K, Xu L, Zou X, Lu F, Li J and Chen G: Wu-Mei-Wan ameliorates chronic colitis-associated intestinal fibrosis through inhibiting fibroblast activation. J Ethnopharmacol 252: 112580, 2020.

45. Zorzi F, Calabrese E, Di Fusco D, De Cristofaro E, Biancone L, Casella S, Palmieri G and Monteleone G: High Smad7 in the early post-operative recurrence of Crohn's disease. J Transl Med 18: 395, 2020.

46. Izzo R, Bevivino G, De Simone V, Sedda S, Monteleone I, Marafini I, Di Giovangiulio M, Rizzo A, Franzè E, Colantoni A, *et al*: Knockdown of Smad7 with a specific antisense oligonucleotide attenuates colitis and colitis-driven colonic fibrosis in mice. Inflamm Bowel Dis 24: 1213-1224, 2018.

47. Monteleone G, Kumberova A, Croft NM, McKenzie C, Steer HW and MacDonald TT: Blocking Smad7 restores TGF-beta1 signaling in chronic inflammatory bowel disease. J Clin Invest 108: 601-609, 2001.

48. Barreiro-de Acosta M, Lorenzo A, Mera J and Dominguez-Muñoz JE: Mucosal healing and steroid-sparing associated with infliximab for steroid-dependent ulcerative colitis. J Crohns Colitis 3: 271-276, 2009.

49. Wen FQ, Liu X, Kobayashi T, Abe S, Fang Q, Kohyama T, Ertl R, Terasaki Y, Manouilova L and Rennard SI: Interferon-gamma inhibits transforming growth factor-beta production in human airway epithelial cells by targeting Smads. Am J Respir Cell Mol Biol 30: 816-822, 2004.

50. Schiffer M, von Gersdorff G, Bitzer M, Susztak K and Böttinger EP: Smad proteins and transforming growth factor-beta signaling. Kidney Int Suppl 77: S45-S52, 2000.

51. Monteleone G, Del Vecchio Blanco G, Monteleone I, Fina D, Caruso R, Gioia V, Ballerini S, Federici G, Bernardini S, Pallone F and MacDonald TT: Post-transcriptional regulation of Smad7 in the gut of patients with inflammatory bowel disease. Gastroenterology 129: 1420-1429, 2005.

52. Troncone E, Marafini I, Stolfi C and Monteleone G: Involvement of Smad7 in inflammatory diseases of the gut and colon cancer. Int J Mol Sci 22: 3922, 2021.

53. Latella G: Redox imbalance in intestinal fibrosis: Beware of the TGFβ-1, ROS, and Nrf2 connection. Dig Dis Sci 63: 312-320, 2018.

54. Cui Y, Zhu C, Ming Z, Cao J, Yan Y, Zhao P, Pang G, Deng Z, Yao Y and Chen Q: Molecular mechanisms by which casein glycomacropeptide maintains internal homeostasis in mice with experimental ulcerative colitis. PLoS One 12: e0181075, 2017.

55. Laudisi F, Dinallo V, Di Fusco D and Monteleone G: Smad7 and its potential as therapeutic target in inflammatory bowel diseases. Curr Drug Metab 17: 303-306, 2016.

56. Speca S, Rousseaux C, Dubuquoy C, Rieder F, Vetuschi A, Sferra R, Giusti I, Bertin B, Dubuquoy L, Gaudio E, *et al*: Novel PPARγ modulator GED-0507-34 levo ameliorates inflammation-driven intestinal fibrosis. Inflamm Bowel Dis 22: 279-292, 2016.

57. Marafini I, Zorzi F, Codazza S, Pallone F and Monteleone G: TGF-beta signaling manipulation as potential therapy for IBD. Curr Drug Targets 14: 1400-1404, 2013.

58. Yamashita A, Inamine T, Suzuki S, Fukuda S, Unoike M, Kawafuchi Y, Machida H, Isomoto H, Nakao K and Tsukamoto K: Genetic variants of SMAD2/3/4/7 are associated with susceptibility to ulcerative colitis in a Japanese genetic background. Immunol Lett 207: 64-72, 2019.